

Interfacial wetting transition in a model with competing multispin interactions

Horacio Ceva

Departamento de Física, Comisión Nacional de Energía Atómica, 1429-Buenos Aires, Argentina

José A. Riera

Physics Department, University of California, Santa Cruz, California 95064

(Received 4 January 1988)

We show the existence of an interfacial or domain-wall wetting transition in the commensurate phase of a model with competing multispin interactions known as the two- plus four-spin model. We perform Monte Carlo simulations from which we detect the wetting transition by measuring the length of the domain walls, the interfacial adsorption, and various standard quantities. The simulations also reveal the presence of two different mechanisms which cause this transition. In addition, we determine the wetting line analytically by using the interfacial transfer matrix formalism.

I. INTRODUCTION

At any finite temperature, several domains can coexist in the ordered phase of two-dimensional spin systems. Such domains correspond to q physically different but equivalent orderings, where q is the degeneracy of the ground state. Systems with short-range competing interactions may exhibit phases with $q \geq 3$. For these systems, a change of temperature T or of the parameter which measures the competition α , may lead to a decomposition of the interface between two domains into two or more interfaces, i.e., one or more of the $q - 2$ remaining domains form a macroscopic slab between those domains. This is the interfacial or domain-wall wetting transition.¹⁻³

Among several models with competing interactions, a great deal of work has been devoted to the axial or anisotropic next-nearest-neighbor Ising (ANNNI) model, which reproduces the essential qualitative features observed in modulated structure materials,^{4,5} such as gases adsorbed on surfaces, intercalated compounds, and magnetic systems. Recently, the existence of a wetting transition in the modulated (2,2) antiphase of the two-dimensional ANNNI model has been demonstrated.⁶ In Ref. 6, it has been argued that this wetting transition is a first-order one, but this fact remains controversial.⁷ Similar wetting phenomena have been found in the various commensurate phases of the two-dimensional ANNNI model in a field.^{7,8}

More recently, it was found that there is an abrupt change in the anisotropy of growth of ordered domains following a quench from the disordered state to a low-temperature nonequilibrium state as one crosses the wetting line, in the ANNNI model with both Glauber and Kawasaki dynamics^{9,10} and in the three-state chiral clock model with Glauber dynamics.¹¹

Another family of spin models which exhibit modulated phases has been considered. In these models, there is

a competition between multispin interactions along a given axis of an hypercubic lattice.^{12,13} Models with multibody interactions are applicable in various fields, and in particular, three- and four-spin interactions successfully describe some magnetic systems.¹⁴ On the theoretical side, the models with multispin interactions in one direction, introduced by Debierre and Turban,¹⁵ has been studied with a variety of techniques including Monte Carlo (MC) simulations,^{16,17} in order to determine the nature of the phase transitions and the universality classes. The phase diagram of a particular competing multispin interactions model, known as the two- plus four-spin model, has been found to be very similar to that of the ANNNI model with ferromagnetic, paramagnetic, and commensurate phases, the latter with an eightfold degeneracy. The main qualitative difference between both models is the absence of an incommensurate phase in the two- plus four-spin model, as has been suggested in a study on its quantum analog.¹⁵

In this article we present some result of a study of wetting transitions in the commensurate phase of the two-plus four-spin model. The interest of this study, apart from the interest in multispin interactions pointed above, is to determine the effects on the wetting transition of a degeneracy of the ground state higher than that of the ANNNI model. Besides, there are probably other effects due to the first-order phase transition which is believed to occur when the four-spin interaction is much greater than the competing nearest-neighbor interaction along the same direction.¹⁶

In Sec. II we define the model, briefly review its bulk properties, and show all the possible domain walls together with their ground-state excess energies. In Sec. III, we present a MC study limited to the determination of some points of the wetting line and show some qualitative features of the transition. Then, in Sec. IV, we obtain some analytical results using the interfacial approximation. In Sec. V we state our conclusions and suggest some possible extensions of this work.

II. MODEL, PHASES, AND INTERFACES

The two- plus four-spin model is defined by the Hamiltonian

$$H = -J_0 \sum_{i,j} s_{ij} s_{ij+1} - J_1 \sum_{i,j} s_{ij} s_{i+1j} + J_2 \sum_{i,j} s_{ij} s_{i+1j} s_{i+2j} s_{i+3j}, \quad (2.1)$$

where the sums extend over the sites of a rectangular lattice with Ising spins $s_{ij} = \pm 1$. The indices i and j correspond to the x and y directions, respectively. We shall only consider the region $J_0, J_1, J_2 \geq 0$, and we adopt the usual parametrization of the ANNNI model: $J_1 = (1 - \alpha)J_0$ and $J_2 = \alpha J_0$ ($0 \leq \alpha \leq 1$). The $p \times 1$ uniaxial commensurate phase, for which the competition between interactions along the x axis is relevant, occurs for $\alpha \geq \frac{1}{3}$ (Fig. 1). In this model, p , the length of an elementary structure of the superlattice in units of the underlying lattice spacing, is equal to four. The commensurate phase is a (3,1) antiphase (the structures of the ground state are formed by the three layers of spins "up" followed by the one layer of spins "down," and so on). Since the up-down symmetry is not broken, the ground state has an eightfold degeneracy.

The 4×1 structures that correspond to the possible ground states may be separated into two classes as A: + + + -, B: + + - +, C: + - + +, and D: - + + +; and A*: - - - +, B*: - - + -, C*: - + - -, and D*: + - - -. Within each class, a given structure may be changed to another by a discrete phase shift. Of course, this is not possible for structures belonging to different classes. This is an important difference with respect to the ground states of the ANNNI model, and it leads to a more complicated behavior of the wetting transition. These two disjoint

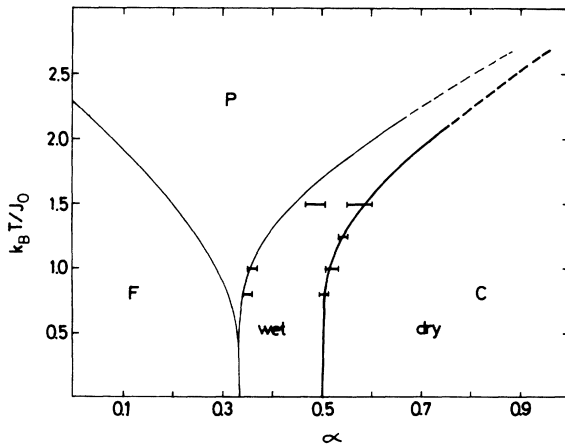


FIG. 1. Phase diagram of the two- plus four-spin model. Light solid curves are the phase boundaries of the ferromagnetic (F), the paramagnetic (P), and the commensurate (C) phases. The heavy solid line indicates the wetting transition. All these curves were obtained from the interfacial approximation (see Sec. IV). The crosses are our MC results. Their approximate error bars are also shown.

classes of $p = 4$ structures each lead to nine distinct types of physically nonequivalent domain walls. These walls, together with their ground-state excess energies—which will be defined in Eq. (4.2)—are given in Table I. The use of Eq. (4.2) introduces some artificial differences in this classification. That is, the wall between B and C states, denoted B|C ("wall 8"), should be included together with A|B and C|D as "light" walls (wall 7), and the wall C|B (wall 8) with B|A and D|C as "heavy" walls (walls 9). In fact, these inclusions are performed in our MC program.

In Table I, we can distinguish three groups of domain walls according to the number of frustrated multispin interactions (f.m.i.): W_1 and W_2 (3 f.m.i.); W_3 , W_4 , W_5 , and W_6 , (2 f.m.i.); and W_7 , W_8 and W_9 (1 f.m.i.).

If we assume that the up-down symmetry is broken, and we take, for example, the case in which the coverage is $\frac{3}{4}$ particles per adsorption site (structures A, ..., D), then the nine types of walls shown in Table I reduce to five: A|D (3 f.m.i.), A|C and C|A (2 f.m.i.), and A|B and D|C (1 f.m.i.).

Of course, there are many possible wetting transitions which can occur by intercalating one or more domains between two other domains. Taking into account the wall energies depicted in Table I, it is easy to determine all the wetting transitions that take place at zero temperature. In this work, we limit ourselves to the study of the wetting transition $W_7 \rightarrow 3W_9$. The reason for this choice is that this transition involves those walls which cost the least energy at $T = 0$ (one frustrated multispin interaction), which are therefore the most abundant. In fact, our MC simulations with full periodic boundary conditions show that the walls 7 and 9 are the most numerous ones.

If one takes the case of coverage $\frac{3}{4}$, this wetting transition would be described as A|B \rightarrow 3D|C (see Sec. III, second case). This transition corresponds, taking into account the usual classification of walls in adsorbate systems, to a decomposition of a light (A|B) wall into three heavy (D|C) walls.

III. MONTE CARLO STUDY

We have performed MC simulations with the standard Metropolis algorithm in order to determine the wetting line and to study the domain-wall process that produce

TABLE I. Domain walls in the commensurate phase. The domain walls obtained by inverting the spins of both phases are not shown.

Type	Domain wall	Energy
W_1	C B*, B C*	$2J_1 + 6J_2$
W_2	A D, D A	$-2J_1 + 6J_2$
W_3	B B*, C C*	$2J_1 + 4J_2$
W_4	A C, B D, C A*, D B*	$J_1 + 4J_2$
W_5	C A, D B, A C*, B D*	$-J_1 + 4J_2$
W_6	A A*, D D*	$-2J_1 + 4J_2$
W_7	A B, C D, B A*, D C*	$J_1 + 2J_2$
W_8	B C, C B, D A*, A D*	$2J_2$
W_9	B A, D C, A B*, C D*	$-J_1 + 2J_2$

this wetting transition. Lattices of sizes $N \times M$, where N refers to the direction x in which there are competing interactions, were used. In general we have taken $N = 64$ and $M = 16$, and in order to study finite-size effects, we also considered $N = 64, M = 8$ and $N = 72, M = 20$. The averages were typically computed over runs which ranged from 6 to 10×10^4 MC steps per spin with sampling every 60 to 100 MC steps per spin. For the $N = 64$ lattices, and near the wetting line, we take from 12 to 16×10^4 MC steps per spin, sampling every 100 MC steps. The boundaries in the x direction were pinned to the A (left boundary) and B (right boundary) structures in order to study the wetting of the A|B light wall (W_7), and periodic boundary conditions were imposed in the y direction.

We computed the length l_i ($i = 1, \dots, 9$) for each of the nine walls shown in Table I. More complicated walls, which we considered as disordered structures, were also computed. We also calculated the number of spins belonging to each of the eight phases A, ..., D* and the interfacial width or interfacial adsorption of the wall A|B (for a precise definition of this quantity, see Ref. 1).

In addition, we have recorded standard quantities such as the nearest-neighbor energies along both the x and y directions, the energy associated with the multispin interaction, and the total energy, and we have calculated their averages and fluctuations. The order parameter computed is

$$\Psi = \frac{1}{MN} \left\langle \sum_{i,j} (s_{ij} - s_{i-2j} s_{i-1j} s_{i+1j}) \right\rangle, \quad (3.1)$$

where $\langle \rangle$ denotes the usual MC average. Each group of four consecutive spins along the x axis contributes $+4$ to Ψ if it belongs to the phases A, ..., D, -4 if it belongs to phases A*, ..., D*, or zero for disordered structures. Ψ is a "good" global order parameter in the sense that the melting transition is detected by the vanishing of Ψ with a corresponding peak in its fluctuations.

The value of α at the wetting transition α_w , for a given temperature, is mainly determined by the vanishing of l_7 , the length of the wall A|B, as the value of the parameter α is lowered from its maximum value $\alpha = 1$ to its value at the melting transition. Simultaneously, l_9 jumps from zero to a value that is near $3M$. These changes in l_7 and l_9 also appear as a peak in the corresponding fluctuations. This picture clearly appears for temperatures $T \leq 1$ (in units of J_0/k_B) and is shown in Fig. 2 (see also Fig. 6). For higher temperatures, we see that l_9 increases and l_7 decreases as α is lowered, but l_7 and l_9 take nonzero values throughout [Fig. 2(b)]. In this case, we determine the wetting transition mainly by the fluctuations of the wall lengths.

Alternatively, we can detect the wetting line from the interfacial adsorption which jumps from a nearly zero value in the dry region to a nonzero value in the wet region (Fig. 3). We see that the interfacial adsorption has two contributions provided by the two mechanisms present at the transition (see the following).

The wetting transition also appears through the global quantities as a slight minimum in the order parameter Ψ

caused by the intrusion of the A* and B* phases, and as peaks in the fluctuations of Ψ , of the energy associated with the two-spin interaction along the x axis and the energy associated with the multispin interactions (Fig. 4).

The wetting transition occurs in the following way. For $\alpha \cong 1$, the wall A|B is almost a straight line. As α is lowered, this interface begins to meander with kinks of one or two lattice spacings to the right. Near the transition, the kinks have three lattice spacings to the right or one to the left, i.e., the W_7 becomes a W_2 (see Fig. 5). For example, at $T = 0.8$ and for $\alpha = 0.505$, slightly on the dry side of the transition line, we have that $l_2 + l_7 = M$, $l_j = 0$ ($j \neq 2$ or 7). We see two possible mechanisms for the wetting transition. In the first of them, the W_7 (or W_2) splits into a W_6 and a W_9 by inverting three consecutive spins [Figs. 5(a)]. Then, by inverting new groups of spins, that is, intruding A* and B* structures, the W_6

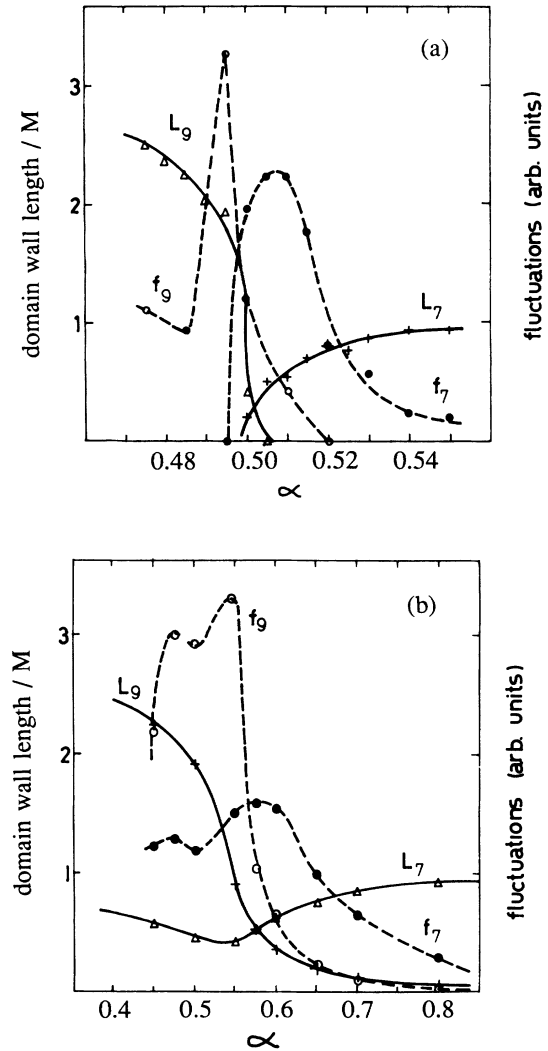


FIG. 2. Behavior of the length of the walls 7 and 9, l_7 and l_9 (solid curves), and of their fluctuations f_7 and f_9 (broken curves), showing the wetting transition (a) at $T = 0.8$ and (b) at $T = 1.5$ (in units of J_0/k_B). In this figure and in the following figures, the full curves must be considered as a guide to the eye.

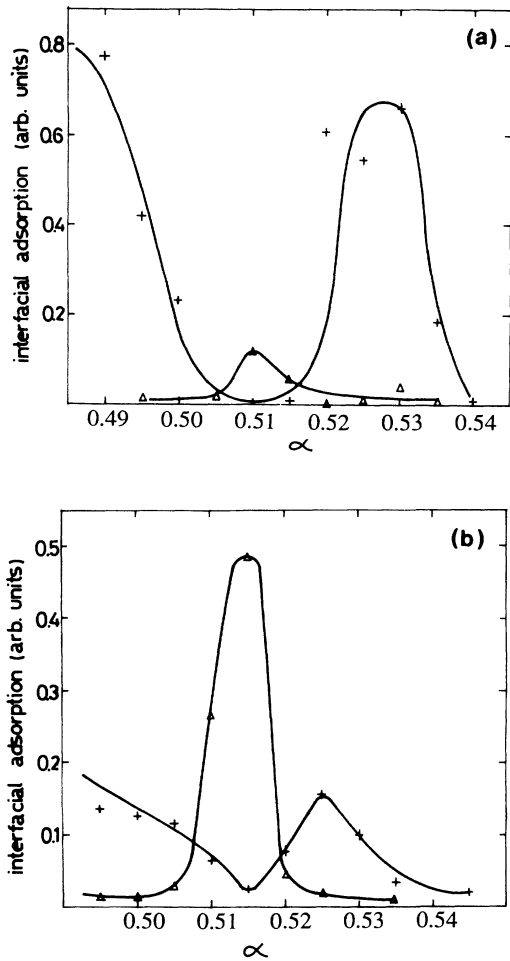


FIG. 3. Interfacial adsorption corresponding to the intruding phases C and D (crosses) and A* and B* (triangles), (a) at $T=0.8$ and (b) at $T=1.5$ (in units of J_0/k_B).

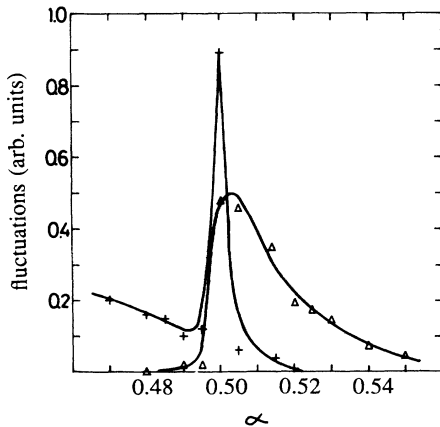


FIG. 4. Fluctuations of the order parameter Ψ (crosses) and of the energy associated with the multispin interactions (triangles), at $T=0.8$.

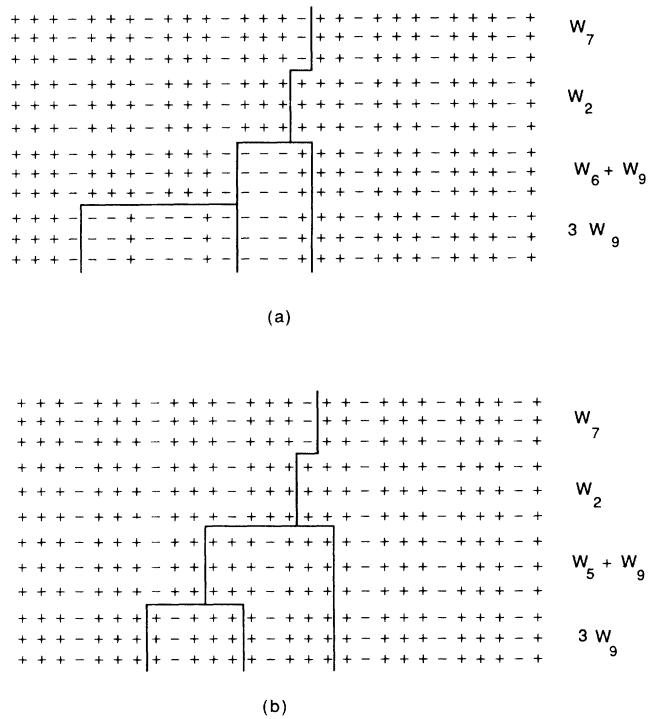


FIG. 5. Possible mechanisms of the wetting transition. In each case, we show, from top to bottom, different stages of the wetting transition that appear as α is lowered. In (a), the intruding phases are A* and B*, and in (b) the intruding phases are C and D.

splits into two new W_9 's and the wet order is reached. There is also an increasing number of disordered structures at this point. This is the mechanism expected from naive combinatorics taking into account Table I, and can be described as $A|B \rightarrow A|B^*|A^*|B$. However, we have found that, for all the temperatures studied ($0.8 \leq T \leq 2.0$), this wet structure is only abundant slightly below the transition point (see Fig. 3). At this point, and for lower values of α , other structures, which appear from the second mechanism, prevail. This mechanism, shown in Fig. 5(b), can be described as

$$A|B \rightarrow A \rightleftharpoons D|C \rightleftharpoons D|B \text{ (two-wall state)}$$

and

$$A|B \rightarrow A \rightleftharpoons D|C \rightleftharpoons D|C \rightleftharpoons D|C \rightleftharpoons B \text{ (three-wall state)},$$

where the double arrows mean that a phase which begins at the left wall as, say C reaches the right wall as D. One can see that the wall $D|B$ (W_5) is the result of the interactions between two neighboring heavy walls $D|C$ (W_9).

For example, at $T=0.8$ and $\alpha=0.495$, slightly on the wet side of the transition line, we have that $l_2=l_7=0$, and the system jumps back and forth between two states, the first with $l_5=l_9=M$ (two-wall state) and the other with $l_5=0$ and $l_9=3M$ (three-wall state). At this point, the system spends approximately equal amounts of time in each state. As α is lowered, the time that the system

stays in the three-wall state increases. Finally, at $\alpha \cong 0.47$, the walls D|C are too far apart to interact and the system reaches a pure three- W_9 state.

Taking into account the important finite-size effects which are present in MC simulations of modulated spin models,^{18,19} we have analyzed the behavior of α at $T=1.0$ for lattices with $N=64$, $M=8$ and 16 and $N=72$, $M=20$. The results, depicted in Fig. 6, show a reasonable convergence to the value predicted by the interfacial approximation.

Starting from various initial configurations, we found important differences in the results due to the presence of metastable states during all the MC runs, especially when the simulation starts with a disordered (high-temperature) configuration. We have preferred to consider dry and wet ordered (low-temperature) starts. At a given temperature, and for each value of α , we start the simulation from the last configuration generated in the run of for the previous value of α . For the wet ordered start, we began with $\alpha=0.485$ and raised α up to 0.600 in steps of 0.005. For the dry start, we followed the inverse sequence.

The possibility of first-order wetting transitions in two-dimensional systems with $p \geq 4$ has been predicted (for a review see Ref. 2). To determine the order of the wetting transition in MC simulations, one may determine the finite-size behavior of the fluctuations in the interfacial adsorption.⁶ Our data at $T=1.0$ with 64×16 lattices show a very peaked behavior in the fluctuations associated with both mechanisms studied above. As it was pointed out in Ref. 7, this implies that extremely long runs and a very fine mesh in the temperatures to be scanned are necessary to get reliable data close to the wetting line. In addition, we should consider other lattice sizes. However, such a systematic finite-size analysis is beyond our present computational possibilities.

IV. INTERFACIAL TRANSFER MATRIX APPROXIMATION

We have also performed a transfer matrix calculation of the excess free energy ("surface tension") of the various interfaces in the solid-on-solid (SOS) approximation

$$\sigma_{A|B} = E_{A|B} - \lim_{M \rightarrow \infty} \frac{k_B T}{M} \ln \sum_{i,j} \exp \left[-\frac{1}{k_B T} \Delta H_{A|B} \{s_{ij}\} \right], \quad (4.1)$$

where, as before, M is the length of the lattice in the direction parallel to the interface,

$$E_{A|B} = \lim_{M \rightarrow \infty} \frac{1}{M} [H_{A|B}^{(0)} - \frac{1}{2}(H_{A|A}^{(0)} + H_{B|B}^{(0)})] \quad (4.2)$$

is the ground-state excess energy of this wall (see Table I), and

$$\Delta H_{A|B} = H - H_{A|B}^{(0)}, \quad (4.3)$$

with H given by Eq. (2.1). $H_{A|B}^{(0)}$, $H_{A|A}^{(0)}$, and $H_{B|B}^{(0)}$ are

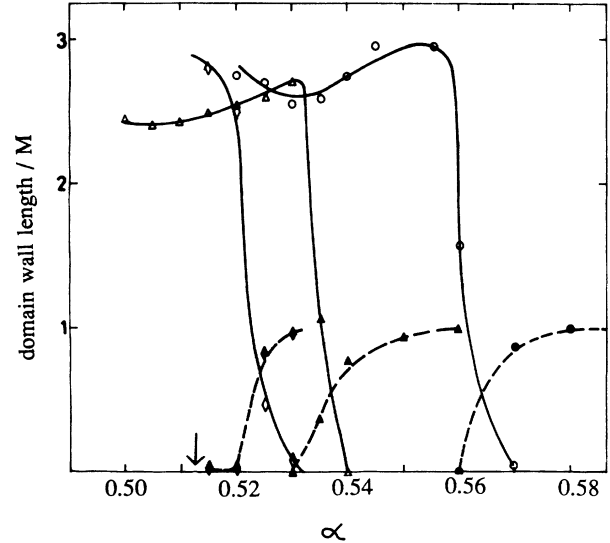


FIG. 6. Finite-size study of the wetting transition at $T=1.0$. The lattice sizes considered are 64×8 (circles), 64×16 (triangles), and 72×20 (diamonds). In all cases, the empty (solid) symbols correspond to the length of the wall 9 (7). The arrow shows the value predicted by the MHZ approximation.

(overhangs and islands excluded) following the procedure developed by Muller-Hartmann and Zittartz²⁰ (MHZ). This method, in principle valid only at low temperatures, has been successfully used to determine the phase boundaries of several two-dimensional models,²¹⁻²⁴ and in some cases, it reproduces the exact value of the critical temperature.²⁰ Moreover, this method has been modified²⁵ to describe the intrusion of a third phase between two other phases in a wetting transition. However, to study the case of two intruding phases, we have followed the original approach, as it was used in Ref. 6 to determine the wetting line in the ANNNI model.

In the interfacial or SOS transfer matrix calculation, the surface tension of a given wall, say $A|B$, is calculated from the expression²⁶

the ground-state energies of the system with boundary conditions in the x direction pinned at (A,B) (the interfacial reference configuration), (A,A) , and (B,B) respectively. The sum in (4.10) runs over the SOS configurations and can be evaluated by transfer matrix methods.

Following the usual interfacial or MHZ approximation, the melting line, phase boundary of the 4×1 phase is determined by the vanishing of the surface tension of the wall with least energy at $T=0$, in our case W_9 . The vanishing of the surface tension occurs in second-order phase transition, which is assumed in the present calcula-

tion.

In order to construct the SOS transfer matrix, we consider the configuration with a W_7 wall, B|A, for example, as the reference configuration. A kink in this wall leads to a W_2 (A|D) configuration which is also included. These are the basic configurations. Then we take all the configurations obtained by shifting the basic configurations in $4n$ lattice spacings, with $-\infty \leq n \leq +\infty$. After performing the usual Fourier transformation of the transfer matrix and taking into account the Perron-Frobenius theorem, we reduce the problem to the diagonalization of the following 2×2 matrix:

$$\tau = \frac{1}{1-x^2} \begin{pmatrix} 1+x^2 & 2xb \\ 2xb & (1+x^2)b^2 \end{pmatrix}, \quad (4.4)$$

where

$$b = \exp \left[\frac{-2\alpha J_0}{k_B T} \right]$$

and

$$x = \exp \left[\frac{-2J_0}{k_B T} \right].$$

In this expression of τ we have already extracted the energy of the reference configuration. Finally, we obtain the W_9 surface tension

$$\sigma_9 = 3\alpha - 1 - \frac{k_B T}{J_0} \ln \lambda, \quad (4.5)$$

where λ , the largest eigenvalue of τ , is

$$\lambda = \frac{1}{2(1-x^2)} \left\{ (1+x^2)(1+b^2) + [(1+x^2)^2(1-b^2)^2 + 16x^2b^2]^{1/2} \right\}. \quad (4.6)$$

The result obtained by setting σ_9 equal to zero is depicted in Fig. 1. These values compare satisfactorily well with MC results at low temperatures. At $\alpha=1$, the pure multispin model, we obtain the value $T=2.923$ for the transition point, considerably higher than the exact one $T \simeq 2.296$. Similar behavior of the interfacial approximation has been found in previous calculations for Ising models with three-spin interactions and second- and third-nearest neighbor interaction.^{23,24} Moreover, one should recall that some authors^{16,17} have found that the transition at $\alpha=1$, $T \simeq 2.269$ is a first-order one.

In Fig. 1, we have also included, for completeness, the phase boundary of the ferromagnetic phase, obtained with the MHZ approximation. In this case, this approximation exactly reproduces the Ising critical point $T_c \simeq 2.296$, which corresponds to $\alpha=0$.

The wetting line is determined from the condition

$$\sigma_7 = \sigma_9^{(3)}, \quad (4.7)$$

where σ_9 is the surface tension of the W_9 interface and $\sigma_9^{(3)}$ is the excess free energy of the system with three W_9 's. The only basic configuration taken into account for the construction of the transfer matrix of σ_7 is a configuration with a W_7 . Following the same procedure

sketched for the σ_9 , we obtain

$$\sigma_7 = 1 + \alpha - \frac{k_B T}{J_0} \ln \frac{1+x^2}{1+x^2}. \quad (4.8)$$

The estimate of $\sigma_9^{(3)}$ is somewhat more involved, because in addition to the three noninteracting W_9 configurations, one should consider configurations in which two out of the three W_9 's are interacting (see Fig. 5). However, the leading eigenvalue of the SOS transfer matrix corresponds to the configurations with three noninteracting W_9 's. Equation (4.7) then reduces to

$$\sigma_7 = 3\sigma_9. \quad (4.9)$$

Finally, taking into account (4.5), (4.6), (4.8), and (4.9), one obtains the results shown in Fig. 1.

V. CONCLUSIONS

We have determined a domain-wall wetting transition in a competing multispin model in which a single interface decomposes into three interfaces due to the intrusion of two new phases between the older ones. The most interesting new feature compared with a similar wetting transition which occurs in the ANNNI model is the existence of two very different mechanisms that cause the transition. We can conjecture that this is due to the higher degeneracy of the ground state of the two- plus four-spin model. It would be worthwhile, from the numerical point of view, to study the interfacial adsorption associated with each mechanism in greater detail and to determine the order of the wetting transition. The relation between Ψ (Fig. 4) and the interfacial adsorption related to the A^* and B^* is another point which should be clarified. From the analytical point of view, with a transfer matrix formulation in the Hamiltonian limit which can include the processes shown in Fig. 5, one could attempt to explain the behavior of the interfacial adsorption shown in Fig. 3. It is possible that the presence of two regions, dry and wet, in the commensurate phase leads to differences in the growth of the ordered domains when quenching from the disordered, high-temperature phase to the commensurate phase. Some preliminary studies with Monte Carlo simulations with Glauber, i.e., nonconserved order parameter dynamics seem to indicate that the growth of order could be influenced by the evolution of three- and four-rayed vertices, the latter formed by heavy (W_9) walls which are more abundant near equilibrium in the wet region. Far from equilibrium, there are also W_9 's in the dry region so the vertex mechanism could be the same in both regions. This is an interesting open question which, together with the dynamics of the wetting transition itself, would deserve an extensive study.

ACKNOWLEDGMENT

One of the authors (J.A.R.) received support from the Consejo Nacional de Investigaciones Científicas y Técnicas (CONICET) of Argentina.

- ¹I. Sega, W. Selke, and K. Binder, *Surf. Sci.* **154**, 331 (1985).
²M. E. Fisher, *J. Stat. Phys.* **34**, 667 (1984).
³D. A. Huse, A. Szpilka, and M. E. Fisher, *Physica* **121A**, 363 (1983).
⁴P. Bak, *Rep. Prog. Phys.* **45**, 587 (1982).
⁵W. Selke, in *Modulated Structure Materials*, edited by T. Tsakalakos (Nijhoff, Boston, 1984).
⁶T. Ala-Nissila, J. Amar, and J. D. Gunton, *J. Phys. A* **19**, 717 (1986).
⁷P. Rujan, W. Selke, and G. Uimin, *Z. Phys. B* **65**, 235 (1986).
⁸P. Rujan, G. Uimin, and W. Selke, *Phys. Rev. B* **32**, 7453 (1985).
⁹T. Ala-Nissila, J. D. Gunton, and K. Kaski, *Phys. Rev. B* **33**, 7583 (1986).
¹⁰T. Ala-Nissila and J. D. Gunton, *J. Phys. C* **20**, L387 (1987).
¹¹J. M. Houlrik and S. J. Knak Jensen, *Phys. Rev. B* **34**, 7828 (1986).
¹²K. A. Penson, *Phys. Rev. B* **29**, 2404 (1984).
¹³M. Kolb and K. A. Penson, *Phys. Rev. B* **31**, 3147 (1985).
¹⁴U. Falk, A. Furrer, H. U. Gudel, and J. K. Kjems, *Phys. Rev. Lett.* **56**, 1956 (1987).
¹⁵J. M. Debierre and L. Turban, *J. Phys. A* **16**, 3571 (1983).
¹⁶F. C. Alcaraz, *Phys. Rev. B* **34**, 4885 (1986).
¹⁷H. W. J. Blote, A. Compagner, A. Hoogland, P. A. M. Cornelissen, F. Mallezie, and C. Vanderzande, *Physica* **139A**, 395 (1986).
¹⁸W. Selke and M. E. Fisher, *Z. Phys. B* **40**, 71 (1980).
¹⁹W. Selke, *Z. Phys. B* **43**, 335 (1981).
²⁰E. Muller-Hartmann and J. Zittartz, *Z. Phys. B* **27**, 261 (1977).
²¹R. M. Hornreich, R. Liebmann, H. G. Schuster, and W. Selke, *Z. Phys. B* **35**, 91 (1979).
²²J. Kroemer and W. Pesch, *J. Phys. A* **15**, 225 (1982).
²³J. Doczi-Reger and P. C. Hemmer, *Physica* **109A**, 541 (1981).
²⁴P. A. Slotte, *J. Phys. A* **15**, 1507 (1982).
²⁵W. Selke and W. Pesch, *Z. Phys. B* **47**, 335 (1982).
²⁶For a general definition of the surface tension, from which Eq. (4.1) is derived, see, e.g., D. Jasnow, *Rep. Prog. Phys.* **47**, 1059 (1984).